machines

MDPI

Article

Estimation of the Interaction Forces in a Compliant pHRI Gripper

Francisco J. Ruiz-Ruiz [1,*], Cristina Urdiales [2] and Jesús M. Gómez-de-Gabriel [1]

[1] Robotics and Mechatronics Group, Escuela de Ingenierías Industriales, Universidad de Málaga, 29071 Málaga, Spain
[2] Ingeniería de Sistemas Integrados Group, Escuela de Ingeniería de Telecomunicación, University of Málaga, 29071 Málaga, Spain
* Correspondence: fjruiz2@uma.es

Abstract: Physical human–robot interaction (pHRI) is an essential skill for robots expected to work with humans, such as assistive or rescue robots. However, due to hard safety and compliance constraints, pHRI is still underdeveloped in practice. Tactile sensing is vital for pHRI, as constant occlusions while grasping make it hard to rely on vision or range sensors alone. More specifically, measuring interaction forces in the gripper is crucial to avoid injuries, predict user intention and perform successful collaborative movements. This work exploits the inherent compliance of a gripper with four underactuated fingers which was previously designed by the authors and designed to manipulate human limbs. A new analytical model is proposed to calculate the external interaction forces by combining all finger forces, which are estimated by using the gripper proprioceptive sensor readings uniquely. An experimental evaluation of the method and an example application in a control system with active compliance have been included to evaluate performance. The results prove that the proposed finger arrangement offers good performance at measuring the lateral interaction forces and torque around the gripper's *Z*-axis, providing a convenient and efficient way of implementing adaptive and compliant grasping for pHRI applications.

Keywords: physical human–robot interaction; underactuated grippers; kinodynamic finger model; proprioceptive force sensing; interaction force calculation

Citation: Ruiz-Ruiz, F.J.; Urdiales, C.; Gómez-de-Gabriel, J.M. Estimation of the Interaction Forces in a Compliant pHRI Gripper. *Machines* **2022**, *10*, 1128. https://doi.org/10.3390/machines10121128

Academic Editors: Shuai Li, Dechao Chen, Mohammed Aquil Mirza, Vasilios N. Katsikis, Dunhui Xiao and Predrag S. Stanimirovic

Received: 26 October 2022
Accepted: 25 November 2022
Published: 28 November 2022

1. Introduction

Physical human–robot interaction (pHRI) is a unique blend of human–robot interaction (HRI) where robots interact physically with humans [1–3]. With the development of cobots and force control schemes, this research topic of robotics has gained importance over the years [4]. In some pHRI cases, robots and humans work in close proximity without engaging in direct physical contact (e.g., object handover [5] or collaboration in manufacturing activities [6]). Physical cooperation implies that both the human and robot contribute to a common task, so safety and ergonomics become a priority [7]. In these cases, humans provide cognitive capabilities (goal setting and decision making), while robots provide power and precision [8]. Recently, there has been a trend toward applications involving contact between humans and robots [9,10]. In this method, tasks like co-carrying of solid objects [11], robotic balance assistance [12] or collaborative tooling [13,14] require a proper estimation of the human intention, which is usually accomplished through analysis of the human–robot interaction forces. In general, in applications such as rescues, human augmentation, rehabilitation or assistance, robots not only need to touch humans but even need to initiate contact sometimes [15–17]. Although some robots rely on special terminals to touch humans (e.g., [18,19]), the general approach uses underactuated fingered grippers. These grippers are fit for various tasks, such as manipulating human limbs [20]. Fully robot-initiated contact presents significant uncertainty. First, the human pose and predisposition are not necessarily constrained. That aside, users might not comply to

collaboration and even refuse interaction. In these cases, it is essential to capture and interpret interaction forces to adapt contact to users' needs and desires or to cease contact if needed. Gripper control often relies on visual and range data to accommodate users' preferences to the system goals. However, when robots operate close to humans, occlusions and noise generate significant uncertainty in many situations. In these cases, embedded contact or force sensors in the gripper may be preferable.

There are differences in interaction forces when grasping human limbs as opposed to handling stand-alone objects. Forces at the gripper when handling single objects are due to the inertial, gravitational, and external contacts. When handling human limb forces caused by the remaining parts of the human's or user's body are added, the dynamic and kinematic constraints of the body have to be taken into account [21]. Additionally, if the human is active, he or she can collaborate with or oppose the robot's motion. Measuring these forces is key to estimating the level of human agreement or disagreement and to accommodating shared motion.

Interaction forces may be sensed by using robot arms with force or torque sensors, adding pressure sensors at the fingers or by simply including proprioceptive sensing in a compliant gripper. Some approaches rely on adding commercial force or torque sensors to the robot's wrist, but they are weak against impact and noise, expensive and require extra data acquisition and processing [22]. Other works provide force sensing to grippers by adding pressure sensing with different technologies, including pneumatic pressure chambers [23]. Some recent robot arms (e.g., those of Kuka Lbr and Franka Emika Panda) already include joint torque sensors, providing model-based end effector force estimation but at an extra cost and with a limited payload. Many cobots implement safe human collaboration based solely on limits on the actuator current. For fluid interaction, though, it could be convenient to use the force readings at the fingers—which are used to ensure grasping force control—to estimate the external forces generated by the human. Finger force estimation may help to reduce the pressure accommodating the surfaces of the fingers to the skin surface and to limit grasping forces which require additional sensing capabilities at the fingers.

There are different approaches to measuring the interaction forces in grippers equipped only with proprioceptive sensors for pHRI. Dollar [24] proposed a gripper equipped with fingers with compliant joints, but instead of joint sensors, it relied on large piezoelectric sensors on the contact surfaces for successful grasping. Later, in [25], they presented an underactuated gripper with tendon-driven underactuated fingers (iRobot-Harvard-Yale fingers) with compliant joints that included passive joint angle measurement and an optical sensor to estimate the rubber joints' bending plus a pressure sensor array. The main drawback of this approach is reportedly poor control of the applied forces. The gripper in [26] was based on an elastic tendon and a piezoresistive force sensor, and it employs an artificial neural network for slippage prevention control. Salvietti et al. [27] proposed a cost-effective underactuated gripper for pHRI where robots are not expected to manipulate humans but objects in cooperative tasks. A previous work by the authors in this field already relied on processing proprioceptive information obtained from the joint passive phalanxes and data from the actuator. Instead of an analytical model, machine learning (ML) was used to estimate the interaction forces [28]. However, the resulting ML model had limited accuracy due to actuator frictions. Thus, in [20], the design was adapted to obtain an analytical model of the force exerted by a finger thanks to the introduction of the elastic component, a full set of high-resolution joint sensors and more precise mechanical components.

This work presents an analytical model to calculate the interaction forces during direct human limb manipulation by combining the force information of all four adaptive underactuated fingers in a low-cost compliant gripper with elastic links designed by the authors and presented in [20]. The gripper (see Figure 1) has four adaptive underactuated fingers developed under the rigid links approach [29]. One of the links has been replaced by an elastic one to provide passive compliance. Aside from that, it includes high-resolution joint sensors in the passive joints to measure compliance and compute the torques, using

capture data to estimate the contact forces based solely on tactile information at the gripper level. The main novelty of the proposed work with respect to previous approaches is that the authors of [20] covered the gripper design and the analytical model of force exerted by a single finger. In this work, equations are proposed to combine the forces in each of the four fingers of the gripper so the interaction forces may be analytically calculated. Interaction forces, as mentioned earlier, can be used to estimate intention and to accommodate to human motion.

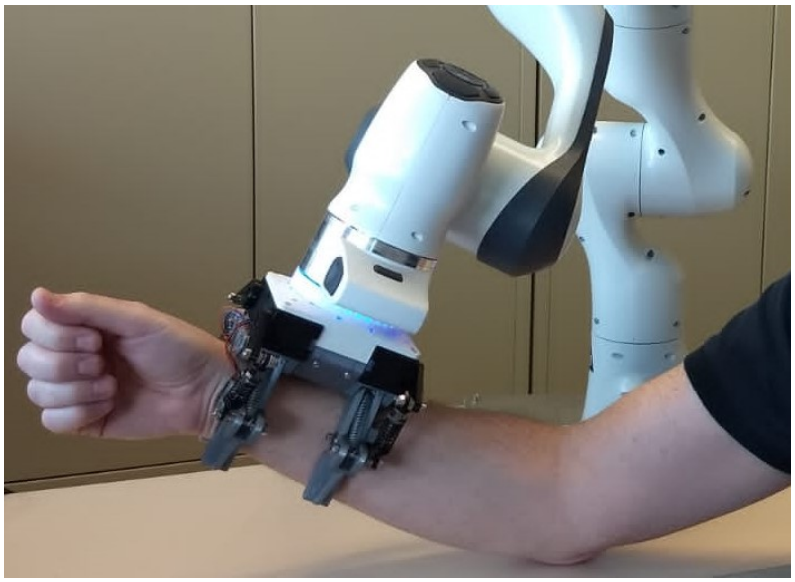

Figure 1. The proposed compliant gripper allows for safe and measurable physical human–robot interaction while underactuated fingers accommodate to a human arm.

The remainder of this paper is organized as follows. The following section briefs the gripper design and the dynamic model of the fingers proposed in [20]. Section 3 describes the interaction force estimation process, which is the main novelty of this work. Section 4 presents experiments conducted to evaluate the accuracy of the estimated forces, and the results are discussed in Section 5. Finally, Section 6 presents the conclusions and possible lines of future research.

2. Underactuated Gripper for Human Manipulation

The main purpose of the gripper is to handle human upper limbs, so every finger was designed by considering the size of the distal section of a human forearm. Due to the soft surface of the human limb, two phalanxes were enough to provide a good balance between adaptation and mechanical complexity. Additionally, a four-finger configuration was adopted to provide a comfortable grasp, as can be seen in Figure 1. To provide accommodation for different arm shapes and roll angle grasping variations, an underactuated approach was used. To avoid interference with the human skin, instead of using tendon-driven mechanisms, the fingers were based on the rigid link approach [29], replacing the link that pushes from the outer side of the gripper with a compression spring. Thus, a multi-bar mechanism was employed to transmit the force from the actuator to the phalanxes. To estimate the relationship between the actuator torque and the forces at the phalanxes, the actual length of the spring had to be computed, so two absolute encoders were added at the passive joints of the phalanxes. This approach led to a finger capable of adapting to the human limb, driven by a single actuator and estimating the closing and opening force applied by the gripper and the external interaction forces caused by the human. In Figure 2, the differences between the rigid links approach and the new compliant design are shown.

A previous prototype of the underactuated gripper designed for human manipulation (Figure 2a) was presented by the authors in [30]. The first prototype was composed of two rigid underactuated fingers without added mechanical compliance. Thanks to the

angular sensor placed in the second phalanx and the actuator feedback, a machine learning model was trained to make an approximate estimation of the human interaction forces [28]. Nevertheless, the actuator's torque estimation was made through current sensing, which could induce some errors since the actuator had a gearbox with a considerable reduction ratio. Aside from that, due to the rigidity of the finger, active compliance control strategies had to be designed and implemented for safe human grasping.

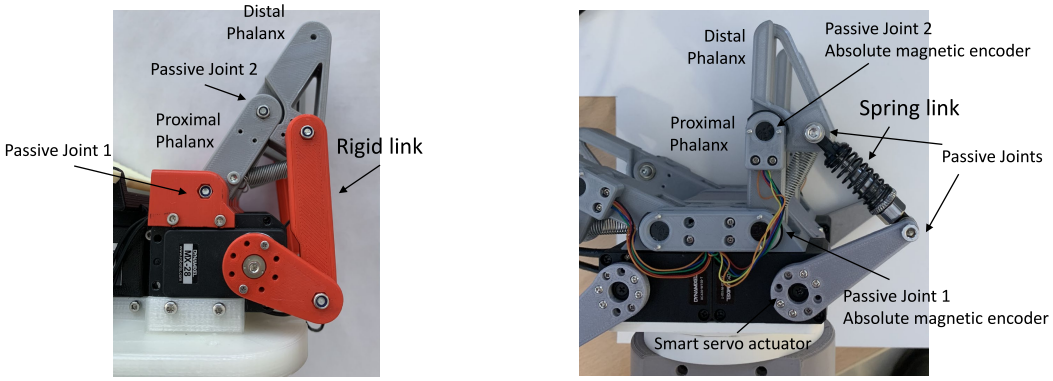

(**a**) (**b**)

Figure 2. Comparison between common underactuated fingers using the rigid link design (**a**) and the new compliant finger that replaces the external link with a compression spring and adds passive joint measurement to estimate the interaction forces (**b**).

To overcome these issues and improve the grasping force sensing capabilities, an improved version of the gripper was designed and presented in [20]. In this design, one rigid link in each of the underactuated fingers was replaced by a spring (see Figure 2b), adding passive compliance to the finger. A four-fingered gripper was implemented to provide a better grasp of the human upper limb, and the control electronics of the gripper were embedded in the gripper's base. The angular sensors placed at the phalanxes (O_1 and O_2 joints) allow for the computation of all joint angles and the spring compression. Moreover, the addition of a compliant link in the kinematic chain of the finger provides a direct measurement of the torque exerted by the actuator, allowing for a more accurate computation of the kinetostatic model of the finger.

Kinetostatic Model of the Compliant Finger

In the model proposed in [20], it is assumed that physical contact between the human and the surface of the phalanxes occurs at points located at distances c_1 and c_2 (see Figure 3). The addition of an elastic link with variable length and the compression spring (S_2) in the kinematic chain of the finger add a new degree of freedom (DOF) to the system (the finger is a six-DOF mechanism which has five rotational joints and one prismatic joint). By replacing S_2 with a rigid link of the same length c at each time instant, the finger can be simplified to a multi-bar mechanism. As all link lengths and the angular positions of the phalanxes and the servo lever are known, c and the length h of the return spring (S_1) can be computed as follows:

$$\begin{cases} h = \sqrt{a^2 + b^2 + 2 \cdot a \cdot b \cdot \sin(\theta_2)} \\ \theta_h = \theta_1 - \arcsin\left(\frac{b}{h} \cdot \cos(\theta_2)\right) \\ c = \sqrt{g^2 + h^2 - 2 \cdot g \cdot h \cdot \cos(\theta_h - \theta_g)} \\ \theta_c = \pi + \theta_g - \arcsin\left(\frac{h}{c} \cdot \sin(\theta_h - \theta_g)\right) \end{cases}, \quad (1)$$

where g is the length of the line O_1-O_4 and θ_g is its angular position:

$$\begin{cases} g = \sqrt{e^2 + d^2 + 2 \cdot e \cdot d \cdot \cos(\theta_a + \gamma)} \\ \theta_g = \arcsin\left(\frac{d}{g} \cdot \sin(\theta_a + \gamma)\right) - \gamma \end{cases}. \tag{2}$$

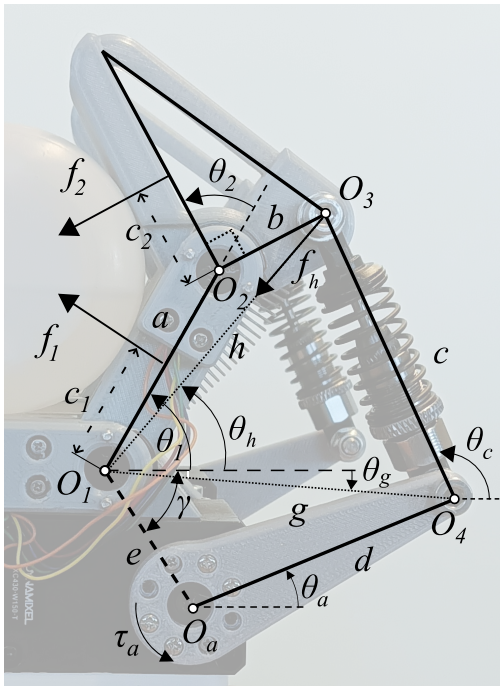

Figure 3. Five-bar model of the finger used for force estimation. The lengths of bars a, b, e and d are known, and as θ_a, θ_1 and θ_2 are measured, the lengths of the elastic link c and the return spring h and the distance g can be computed.

On the other hand, the force transmitted by the spring S_x (with $x = 1, 2$) is given by

$$f_{Sx} = k_{Sx} \cdot (l_{Sx_R} - l_x), \tag{3}$$

where k_{Sx} and l_{Sx_R} are the elastic constant and the length in the resting position of the spring x, respectively, and l_x (with $l_x = h, c$) is the actual length of S_x. Hence, the actual torque at the actuator τ_a is given by

$$\tau_a = d \cdot f_{S2} \cdot \cos(\alpha), \tag{4}$$

where α is the relative orientation between S_2 and the normal to the servo lever, computed as

$$\alpha = \theta_c - (\theta_a + \frac{\pi}{2}). \tag{5}$$

The static equilibrium of the mechanism can be computed by applying the principle of virtual work such that

$$J_n^T \boldsymbol{f}_n + J_a^T \tau_a + J_2^T f_h = 0, \tag{6}$$

where J_n, J_a and J_2 are the contact points, the actuator and the return spring Jacobian matrices, respectively, $\boldsymbol{f}_n = [f_{n1}, f_{n2}]^T$ is the vector of the normal contact forces at the phalanxes, τ_a is the actuator torque obtained in Equation (4) and f_h is the force exerted by

spring S_1 obtained in Equation (3). Finally, the normal contact forces at the phalanxes can be obtained by solving Equation (6):

$$\boldsymbol{f}_n = -J_n^{-T}\left(J_a^T\,\tau_a + J_2^T\,f_h\right). \tag{7}$$

Please refer to [20] for more information about the derivation of the model. With this model, the Cartesian forces at the contact points in the designed gripper can be obtained, and this information can be used to measure both the grasping and interaction forces between the robot and the grasped object or person.

3. Computation of the Interaction Forces

During object manipulation, the only forces involved in the gripper are the grasping forces and the dynamic behavior of the object. In contrast, when grasping a human limb, two possible scenarios may happen:

- The human is completely passive (i.e., the human does not apply any force). In this scenario, then the gripper is exerting a static grasp, and since the human limb is in equilibrium, the forces applied by all fingers are the same.
- The human applies forces to the gripper. In this situation, to maintain the grasp of the human limb, some fingers have to apply more force to compensate for human interaction.

During human limb manipulation, a human can apply forces (i.e., interaction forces) on purpose. The interaction forces can be used to provide robot accommodation to the movements of the humans, shared control, user intention estimation or just as a safety stop or release detection. In this section, these interaction forces are extracted from the Cartesian forces discussed in Section 2.

With the current finger arrangement (see Figure 4), where all the axes are parallel to the Y-axis, it is clear that forces along such an axis did not produce any effect over the fingers' springs, so they could not be measured. Nevertheless, this configuration maximized the measurement sensitivity along the X-axis, and poor sensitivity along the Z-axis was expected, as the gripper was designed to allow the human to release it easily. Moreover, as the gripper had two parallel couples of fingers, it would also be possible to estimate the torques around the Z-axis.

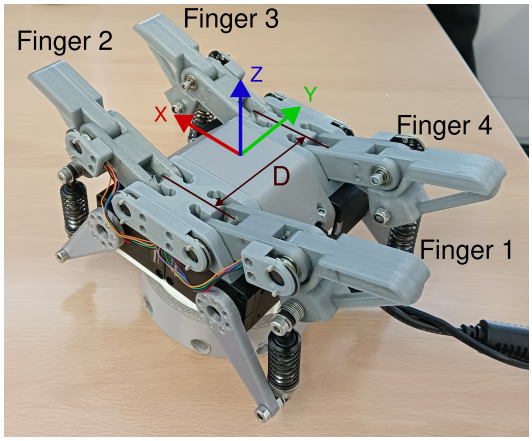

Figure 4. Prototype of the four-fingered gripper with elastic links with the finger numbering and the gripper frame used in the experiments. The two pair of fingers are separated by a distance D.

From this point forward, individual Cartesian forces relative to the gripper Cartesian frame are referred to as $f_{i,j}$ for every phalanx $i = 1, 2$ and finger $j = 1, 2, 3, 4$. Likewise, f_{i,j_x} is the component of the force along the X-axis.

By applying the equilibrium of the forces along the gripper's X-axis, the lateral interaction forces can be obtained as the sum of the horizontal components of the forces f_1 and f_2 for every finger:

$$\begin{aligned} f_{int_x} = & f_{1,1_x} + f_{1,2_x} + f_{4,1_x} + f_{4,2_x} + \\ & f_{2,1_x} + f_{2,2_x} + f_{3,1_x} + f_{3,2_x}. \end{aligned} \tag{8}$$

Similarly, the forces along the gripper's Z-axis are computed as the sum of the vertical components of the forces f_1 and f_2 for every finger:

$$\begin{aligned} f_{int_z} = & f_{1,1_z} + f_{2,1_z} + f_{3,1_z} + f_{4,1_z} + \\ & f_{1,2_z} + f_{2,2_z} + f_{3,2_z} + f_{4,2_z}. \end{aligned} \tag{9}$$

Finally, the interaction torque is computed as the difference of the X-axis components of the forces measured in the fingers in the opposing corners (1 and 3 as well as 2 and 4) and its distance to the Z-axis ($D/2$):

$$\begin{aligned} \tau_{int_z} = & \frac{D}{2}((f_{1,1_x} + f_{1,2_x} + f_{3,1_x} + f_{3,2_x}) - \\ & (f_{2,1_x} + f_{2,2_x} + f_{4,1_x} + f_{4,2_x})). \end{aligned} \tag{10}$$

4. Experiments and Results

A gripper with four fingers was implemented using FDM 3D printers in PETG plastic and joints with miniature ball bearings. A total of eight magnetic absolute angular sensors (as5048A from ams-OSRAM AG) with SPI outputs were added to the passive joints of the phalanxes. Each finger had a smart servo actuator (Dynamixel XC430-W150 from Robotis) capable of a maximum torque of 1.6 Nm and a 12-bit angular resolution. A compact version of an Arduino Mega 2560 microcontroller was embedded in the gripper that reads the sensors and communicates with the servos, providing synchronized data logging to the host computer.

To test the performance of the proposed model, the gripper was attached to the flange of a sensitive collaborative robot known as Panda (Franka Emika GmbH, Germany), which is capable of six-axis force sensing and whose readings were taken as the ground truth. During the experiments, forces were extracted from both the proposed model and the Panda robot. A Linux-based computer running ROS was the controller of the experiments. It communicated in real time with both the Panda robot arm and the gripper controller.

Two types of experiments were performed. In the first one, after gripping a volunteer's arm, the robot arm remained static while the person exerted force in different directions. In the second experiment, the volunteer moved his or her arm, and the robot maintained a compliant grip through the trajectory.

4.1. Measurement of the Interaction Forces

The first experiment was designed to evaluate the accuracy of the proposed method for the estimation of interaction forces with the underactuated gripper. The volunteer sat in front of the robot in a comfortable position and placed his or her forearm in the gripper. The actuators of the gripper were commanded with a constant PWM value of 250, grasping the volunteer's forearm. The robot remained still during the experiment to avoid reading of the interaction forces induced by the robot's movement.

Three different tests were performed. First, the volunteer was asked to gradually apply a force in one direction until a maximum force threshold (10 N) was measured by the robot arm and then progressively apply the same force in the opposite direction along the X-axis in both cases. In a second test, the same action was performed, this time along the Z-axis. Finally, the human was asked to rotate his or her arm around the gripper's Z-axis until a maximum torque threshold (1 Nm) was measured to check if the torques were also correctly obtained. During the whole experiment, a real-time graphical representation of the forces

measured by the robot was displayed on a screen to provide a visual feedback reference for the volunteer.

Figures 5a,c show that the forces obtained by the gripper on the X-axis and the torques on the Z-axis followed the ground truth data with a slight deviation. However, the gripper often returned higher values around the peaks. This likely happened because of unmodeled friction. Nevertheless, the differences were not too significant. In terms of error, the estimation of the force in the X-axis presented an RMSE of 1.2 ± 0.54 N (and an MAE of 0.95 ± 0.54 N), whereas the estimations of the torque on the Z-axis presented an RMSE of 0.07 ± 0.0018 Nm (and an MAE of 0.056 ± 0.0018 Nm).

Figure 5b presents the results for the estimation of the lineal forces along the Z-axis. In this case, the proposed model was not reliable, as noted from the significant differences in magnitude between the robot measurement and the estimated value with the gripper model. Due to the properties of the gripper, when the volunteer applied a force in the negative direction of the Z-axis, the phalanxes' configuration changed to release the user, but the spring length remained almost unaltered, as can be seen in Figure 6a,b. On the contrary, when the volunteer applied a force in the positive direction of the Z-axis, the base of the fingers was reached (Figure 6c). At this point, increasing the force had null effect over the fingers (the force was absorbed by the base of the gripper), so it could not be estimated. Nonetheless, it is worth noticing that the measured and estimated forces along the Z-axis were correlated, and the peaks were aligned, meaning that the force direction was correctly obtained and the magnitude, although attenuated, was consistent through the experiment.

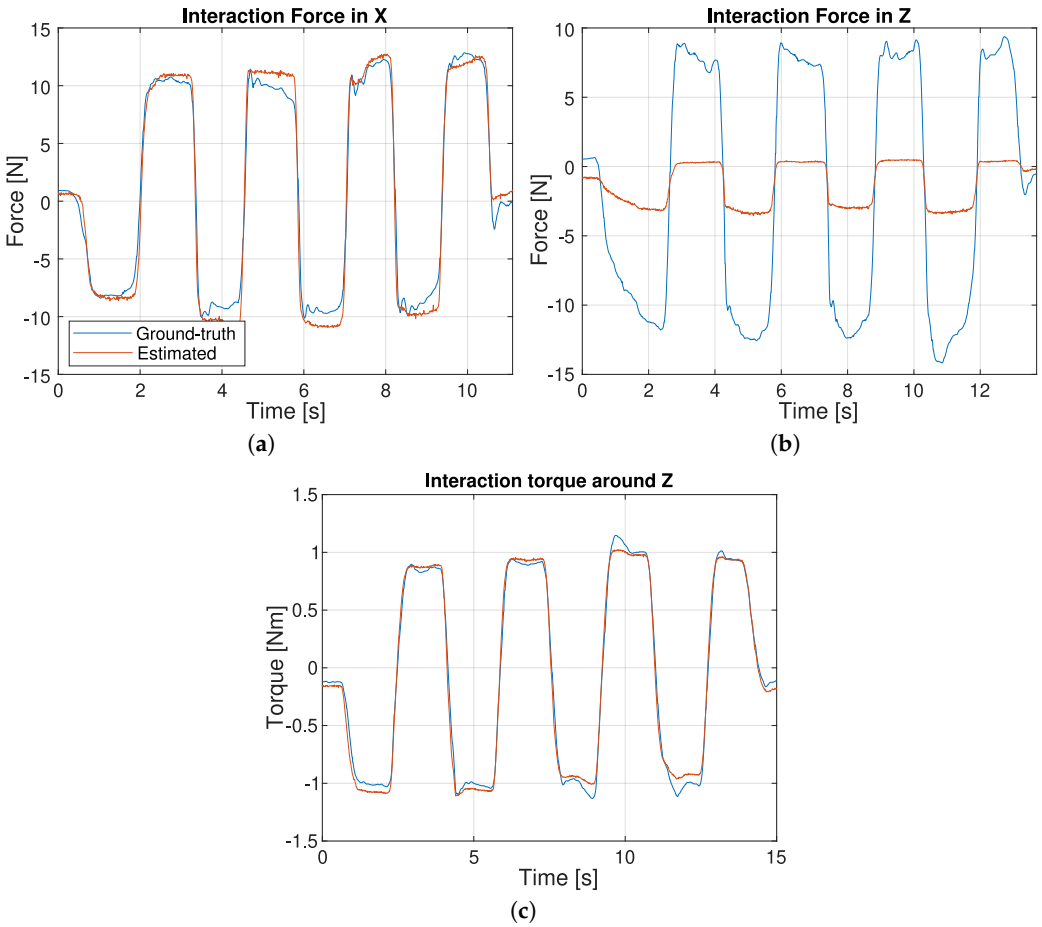

Figure 5. Performance of the estimation of (**a**) lateral ($X-$axis) and (**b**) vertical ($Z-$axis) interaction forces and (**c**) axial interaction torque on $Z-$axis.

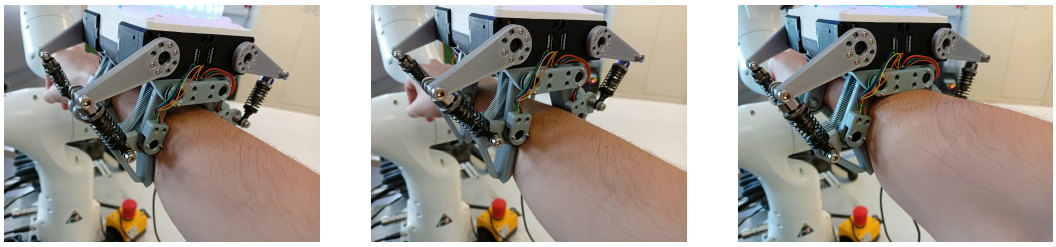

(**a**) (**b**) (**c**)

Figure 6. A volunteer conducting the first experiment along the $Z-$axis. (**a**) The volunteer did not apply any force. (**b**) The volunteer applied a force on the $Z-$axis in the positive direction. (**c**) The volunteer applied a force on the $Z-$axis in the negative direction.

4.2. Active Compliance

In the second experiment, the estimated force or torque was used to achieve active compliance. This time, after the robot gripped the human arm, the volunteer was asked to repeat the same procedure of the previous experiment, but this time, the robot followed the human motion according to the control scheme shown in Figure 7, canceling the interaction forces. This experiment is an example of a practical application of the presented model.

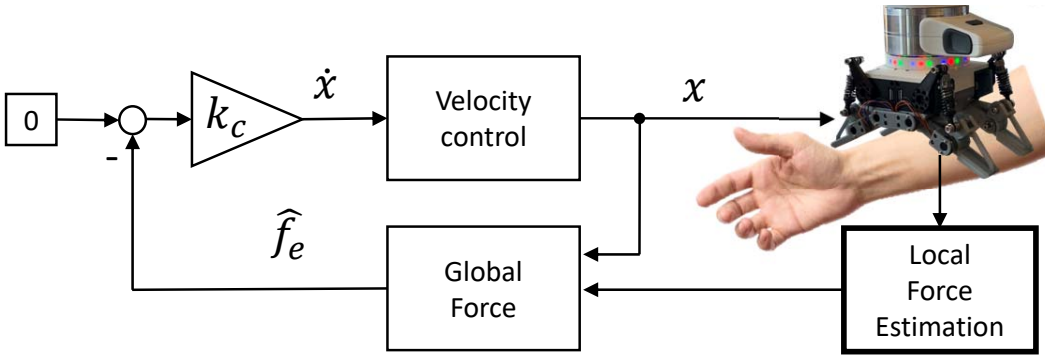

Figure 7. Basic active compliance control. The estimated global Cartesian forces are used to cancel the interaction forces between humans and robots. The velocity of the end effector is proportional to the Cartesian forces, so the robot accommodates the movement of the human.

During these experiments, the volunteer performed a linear motion on the X-axis and a rotation around the Z-axis. Linear motions along the Z-axis were not considered in this experiment due to the inability of the gripper to accurately estimate forces in this direction (as shown in the results of the previous experiment). The results (see Figure 8) include the trajectories of the force computed by the Panda robot arm, used as a ground truth measurement (blue plot), the forces estimated by the compliant gripper (red plot) and the position (green plot) and velocity (purple plot) of the robot effector over time. It can be observed how, in all cases, the force increased steadily until a peak was reached just before the effector reached its target position in both directions. In all presented tests, the grip was always well-adjusted and maintained, regardless of the force magnitude and direction.

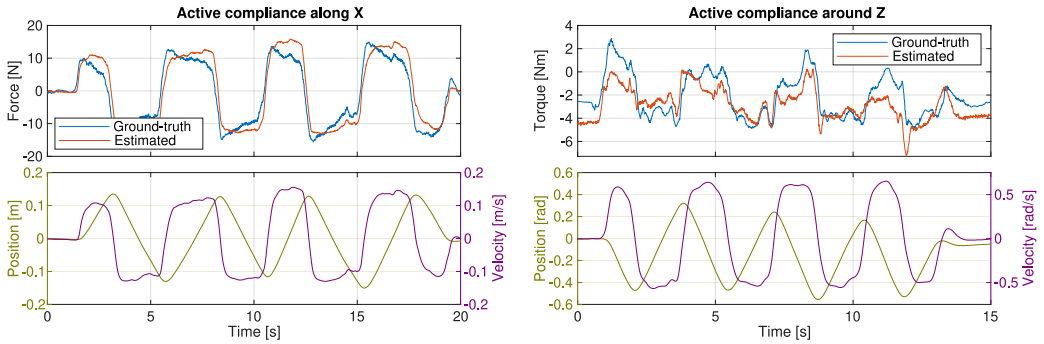

Figure 8. Force or torque measured by the robot and estimated by the gripper, as well as position and velocity of the robot end effector under active compliant control using the force or torque estimated with the presented method on side interaction forces ($X-$axis) (**a**) and around the gripper on the $Z-$axis (**b**).

5. Discussion

The presented method provides external force measurement at the fingers with a proper estimation of the magnitude of the forces in the direction of the main finger actuation (X-axis), and thanks to the four-finger configuration, an estimation of the torque around the Z-axis was also measured. A limitation of the prototype with its current parallel configuration is its inability to measure the interaction forces in the direction of the axes of the phalanxes (Y-axis). The interaction forces in the direction inside the gripper (positive Z-axis) are physically limited by the contact with the palm, and those outside the gripper (negative Z-axis) are detected with a large estimation error.

The passive compliance of the gripper is not only used to measure the forces. It also provides comfort and safety, as the user can release him or herself when needed. The range of measurable forces can be increased with stiffer springs. In this case, the active compliance method can be used to make the interaction with the robot safer and more responsive.

A close approach was taken in [31], where a tendon-driven gripper with underactuated fingers was presented. They implemented a similar reversible linear actuator using a spring. The linear actuator that drives the closing cable has force sensing and control capability. In this way, the finger is compliant, and the effects of the interaction forces at the actuator are measured. However, the configuration of the underactuated section is not monitored, so no estimation of the Cartesian forces can be obtained.

Another related approach [32] provides adaptive underactuation thanks to the fin ray structure of the fingers and intrinsic compliance due to the elasticity of the construction material. The authors developed a model to determine the surface forces based on the structural deformation of the finger beams. In this way, this gripper also provides compliance and force estimation capability. Their approach shows similar limitations in measuring forces along the Y- and Z-axes. Thus far, the proprioceptive information is obtained with the help of an external camera, limiting the practical application of this method.

6. Conclusions

This work presented a novel method to obtain the interaction forces in a low-cost compliant gripper with elastic links, uniquely using the gripper's own sensors. Specifically, the interaction forces are extracted from an analytical model of the Cartesian forces in the gripper during contact. This tactile information is particularly useful in pHRI for complementing visual or range information in close proximity, where the robot and human bodies often provoke occlusions. Although some robot arms already provide force estimation, data extracted from the grasp allow the use of force control schemes in robot manipulators not equipped with force sensors as well.

In order to test the system, the gripper was attached to a commercial, redundant and sensitive robot arm (Panda from Franka Emika). This robot provides force measurement,

which was used as a reference to validate the proposed model. The tests consisted of grasping a human arm and then asking the volunteer to apply different forces or torques on the X- and Z-axes, first keeping the robot arm static and then allowing compliant motion. The results for the forces along the X-axis and torques around the Z-axis were very similar to the reference. However, the amplitude of the forces along the Z-axis returned by the model were smaller than those in the reference, providing an unreliable estimation. This problem was intrinsic to the gripper configuration, as the gripper was explicitly designed to allow humans to release themselves by applying a force on the Z-axis. Yet, the force estimation and ground truth measurement were correlated and quite aligned even in this case.

Depending on the expected dimensions of the human forearm (or other body parts), changes in the design parameters can make the system more sensitive along the Z-axis. Reducing the distance between opposing fingers while increasing the lengths of the phalanxes to avoid a reduction in the diameter of the graspable forearm will make the normal of the contact surfaces more aligned with the gripper's Z-axis. Additionally, changes in the estimation algorithm can be performed to include hard-to-model friction effects. In particular, machine learning methods have been successfully used in previous works.

Future works will focus on studying the trade-off between increasing the force sensing capabilities of the gripper and increasing the passive compliance of the grasp to maximize both variables of force sensing and safety. Moreover, more accurate and safe handling of the human body could be achieved by taking further advantage of the proprioceptive sensing of the gripper and developing methods that provide information on the limb-grasping location. Furthermore, active grasping force control could be implemented in combination with the interaction force estimation to achieve a gentle grasp of the human limb while ensuring the safety of the interaction.

Author Contributions: Conceptualization, F.J.R.-R. and J.M.G.-d.-G.; methodology, F.J.R.-R. and J.M.G.-d.-G.; software, F.J.R.-R.; validation, F.J.R.-R., C.U. and J.M.G.-d.-G.; investigation, F.J.R.-R.; resources, F.J.R.-R. and J.M.G.-d.-G.; writing—original draft preparation, F.J.R.-R., C.U. and J.M.G.-d.-G.; visualization, F.J.R.-R.; supervision, J.M.G.-d.-G.; project administration, C.U. and J.M.G.-d.-G.; funding acquisition, C.U. and J.M.G.-d.-G. All authors have read and agreed to the published version of the manuscript.

Funding: This work was supported by the Universidad de Málaga, project UMA20-FEDERJA-052.

Data Availability Statement: Not applicable.

Conflicts of Interest: The authors declare no conflict of interest.

References

1. De Luca, A.; Flacco, F. Integrated control for pHRI: Collision avoidance, detection, reaction and collaboration. In Proceedings of the 2012 4th IEEE RAS EMBS International Conference on Biomedical Robotics and Biomechatronics (BioRob), Rome, Italy, 24–27 June 2012; pp. 288–295. [CrossRef]
2. Vitiello, N.; Lenzi, T.; Roccella, S.; De Rossi, S.M.M.; Cattin, E.; Giovacchini, F.; Vecchi, F.; Carrozza, M.C. NEUROExos: A Powered Elbow Exoskeleton for Physical Rehabilitation. *IEEE Trans. Robot.* **2013**, *29*, 220–235. [CrossRef]
3. Lee, H.; Kim, W.; Han, J.; Han, C. The technical trend of the exoskeleton robot system for human power assistance. *Int. J. Precis. Eng. Manuf.* **2012**, *13*, 1491–1497. [CrossRef]
4. Bicchi, A.; Bavaro, M.; Boccadamo, G.; De Carli, D.; Filippini, R.; Grioli, G.; Piccigallo, M.; Rosi, A.; Schiavi, R.; Sen, S.; et al. Physical human-robot interaction: Dependability, safety, and performance. In Proceedings of the 2008 10th IEEE International Workshop on Advanced Motion Control, Trento, Italy, 26–28 March 2008; pp. 9–14. [CrossRef]
5. Mizanoor Rahman, S.M.; Wang, Y.; Walker, I.D.; Mears, L.; Pak, R.; Remy, S. Trust-based compliant robot-human handovers of payloads in collaborative assembly in flexible manufacturing. In Proceedings of the 2016 IEEE International Conference on Automation Science and Engineering (CASE), Fort Worth, TX, USA, 21–25 August 2016; pp. 355–360. [CrossRef]
6. Li, S.; Wang, R.; Zheng, P.; Wang, L. Towards proactive human–robot collaboration: A foreseeable cognitive manufacturing paradigm. *J. Manuf. Syst.* **2021**, *60*, 547–552. [CrossRef]
7. Gualtieri, L.; Rauch, E.; Vidoni, R. Emerging research fields in safety and ergonomics in industrial collaborative robotics: A systematic literature review. *Robot.-Comput.-Integr. Manuf.* **2021**, *67*, 101998. [CrossRef]

8. Selvaggio, M.; Cognetti, M.; Nikolaidis, S.; Ivaldi, S.; Siciliano, B. Autonomy in Physical Human-Robot Interaction: A Brief Survey. *IEEE Robot. Autom. Lett.* **2021**, *6*, 7989–7996. [CrossRef]
9. Escobedo, C.; Strong, M.; West, M.; Aramburu, A.; Roncone, A. Contact Anticipation for Physical Human–Robot Interaction with Robotic Manipulators using Onboard Proximity Sensors. In Proceedings of the 2021 IEEE/RSJ International Conference on Intelligent Robots and Systems (IROS), Prague, Czech Republic, 27 September–1 October 2021; pp. 7255–7262. [CrossRef]
10. Magrini, E.; Flacco, F.; De Luca, A. Control of generalized contact motion and force in physical human-robot interaction. In Proceedings of the 2015 IEEE International Conference on Robotics and Automation (ICRA), Seattle, WA, USA, 26–30 May 2015; pp. 2298–2304. [CrossRef]
11. Yu, X.; He, W.; Li, Q.; Li, Y.; Li, B. Human-Robot Co-Carrying Using Visual and Force Sensing. *IEEE Trans. Ind. Electron.* **2021**, *68*, 8657–8666. [CrossRef]
12. Ruiz-Ruiz, F.J.; Giammarino, A.; Lorenzini, M.; Gandarias, J.M.; Gómez-De-Gabriel, J.H.; Ajoudani, A. Improving Standing Balance Performance through the Assistance of a Mobile Collaborative Robot. In Proceedings of the 2022 International Conference on Robotics and Automation (ICRA), Philadelphia, PA, USA, 23–27 May 2022; pp. 10017–10023. [CrossRef]
13. Erden, M.S.; Billard, A. Robotic Assistance by Impedance Compensation for Hand Movements While Manual Welding. *IEEE Trans. Cybern.* **2016**, *46*, 2459–2472. [CrossRef] [PubMed]
14. Villa, N.; Mobedi, E.; Ajoudani, A. A Contact-Adaptive Control Framework for Co-Manipulation Tasks with Application to Collaborative Screwing. In Proceedings of the 2022 31st IEEE International Conference on Robot and Human Interactive Communication (RO-MAN), Napoli, Italy, 29 August–2 September 2022; pp. 1131–1137. [CrossRef]
15. Pons, J.L. *Wearable Robots: Biomechatronic Exoskeletons*; John Wiley & Sons: New York, NY, USA, 2008.
16. Zhao, Z.; Li, X.; Lu, C.; Zhang, M.; Wang, Y. Compliant Manipulation Method for a Nursing Robot Based on Physical Structure of Human Limb. *J. Intell. Robot. Syst.* **2020**, *100*, 973–986. [CrossRef]
17. Feil-Seifer, D.; Mataric, M.J. Defining socially assistive robotics. In Proceedings of the International Conference on Rehabilitation Robotics (ICORR), Chicago, IL, USA, 28 June–1 July 2005; pp. 465–468.
18. Rocon, E.; Belda-Lois, J.M.; Ruiz, A.F.; Manto, M.; Moreno, J.C.; Pons, J.L. Design and Validation of a Rehabilitation Robotic Exoskeleton for Tremor Assessment and Suppression. *IEEE Trans. Neural Syst. Rehabil. Eng.* **2007**, *15*, 367–378. [CrossRef] [PubMed]
19. Jones, K.; Du, W. Development of a massage robot for medical therapy. In Proceedings of the 2003 IEEE/ASME International Conference on Advanced Intelligent Mechatronics (AIM 2003), Kobe, Japan, 20–24 July 2003; Volume 2, pp. 1096–1101. [CrossRef]
20. Ruiz-Ruiz, F.J.; Ventura, J.; Urdiales, C.; de Gabriel, J.M.G. Compliant gripper with force estimation for physical human–robot interaction. *Mech. Mach. Theory* **2022**, *178*, 105062. [CrossRef]
21. Ruiz-Ruiz, F.J.; Gandarias, J.M.; Pastor, F.; Gómez-De-Gabriel, J.M. Upper-Limb Kinematic Parameter Estimation and Localization Using a Compliant Robotic Manipulator. *IEEE Access* **2021**, *9*, 48313–48324. [CrossRef]
22. Petrea, R.A.B.; Bertoni, M.; Oboe, R. On the Interaction Force Sensing Accuracy Of Franka Emika Panda Robot. In Proceedings of the IECON 2021—47th Annual Conference of the IEEE Industrial Electronics Society, Toronto, ON, Canada, 13–16 October 2021; pp. 1–6. [CrossRef]
23. Yang, H.; Chen, Y.; Sun, Y.; Hao, L. A novel pneumatic soft sensor for measuring contact force and curvature of a soft gripper. *Sens. Actuators Phys.* **2017**, *266*, 318–327. [CrossRef]
24. Dollar, A.M.; Jentoft, L.P.; Gao, J.H.; Howe, R.D. Contact sensing and grasping performance of compliant hands. *Auton. Robot.* **2010**, *28*, 65–75. [CrossRef]
25. Odhner, L.U.; Jentoft, L.P.; Claffee, M.R.; Corson, N.; Tenzer, Y.; Ma, R.R.; Buehler, M.; Kohout, R.; Howe, R.D.; Dollar, A.M. A compliant, underactuated hand for robust manipulation. *Int. J. Robot. Res.* **2014**, *33*, 736–752. [CrossRef]
26. Nacy, S.M.; Tawfik, M.A.; Baqer, I.A. A Novel Approach to Control the Robotic Hand Grasping Process by Using an Artificial Neural Network Algorithm. *J. Intell. Syst.* **2017**, *26*, 215–231. [CrossRef]
27. Salvietti, G.; Iqbal, Z.; Hussain, I.; Prattichizzo, D.; Malvezzi, M. The co-gripper: A wireless cooperative gripper for safe human robot interaction. In Proceedings of the 2018 IEEE/RSJ International Conference on Intelligent Robots and Systems (IROS), Madrid, Spain, 1–5 October 2018; pp. 4576–4581.
28. Ballesteros, J.; Pastor, F.; Gómez-de Gabriel, J.M.; Gandarias, J.M.; García-Cerezo, A.J.; Urdiales, C. Proprioceptive Estimation of Forces Using Underactuated Fingers for Robot-Initiated pHRI. *Sensors* **2020**, *20*, 2863. [CrossRef]
29. Birglen, L.; Laliberté, T.; Gosselin, C.M. *Underactuated Robotic Hands*; Springer: Berlin, Germany, 2007; Volume 40.
30. Gandarias, J.M.; Pastor, F.; Muñoz-Ramírez, A.J.; García-Cerezo, A.J.; Gómez-de-Gabriel, J.M. Underactuated Gripper with Forearm Roll Estimation for Human Limbs Manipulation in Rescue Robotics. In Proceedings of the 2019 IEEE/RSJ International Conference on Intelligent Robots and Systems (IROS), Macau, China, 3–8 November 2019; pp. 5937–5942. [CrossRef]
31. Hua, H.; Liao, Z.; Wu, X.; Chen, Y.; Feng, C. A back-drivable linear force actuator for adaptive grasping. *J. Mech. Sci. Technol.* **2022**, *36*, 4213–4220. [CrossRef]
32. Xu, W.; Zhang, H.; Yuan, H.; Liang, B. A Compliant Adaptive Gripper and Its Intrinsic Force Sensing Method. *IEEE Trans. Robot.* **2021**, *37*, 1584–1603. [CrossRef]